Palaeogeography, Palaeoclimatology, Palaeoecology 678 (2025) 113226

Contents lists available at ScienceDirect

Palaeogeography, Palaeoclimatology, Palaeoecology

journal homepage: www.elsevier.com/locate/palaeo

Stable Sr isotopes of fossil dental enamel reflect diet and digestive system differences among sympatric herbivores

Elena Armaroli [a], Razika Chelli Cheheb [b], Anna Cipriani [a,c], Sara Bernardini [a,d], Jan van der Made [e], Isabel Cáceres [f,g], Mohamed Sahnouni [h,b,i,j], Federico Lugli [a,k,*]

[a] MeGic Lab, Department of Chemical and Geological Sciences, University of Modena and Reggio Emilia, Via G. Campi 103, 41125 Modena, Italy
[b] Centre National de Recherches Préhistoriques, Anthropologiques et Historiques (CNRPAH), Algiers, Algeria
[c] Lamont-Doherty Earth Observatory of Columbia University, 61 Route 9W, 10964 Palisades, NY, USA
[d] Department of Cultural Heritage, University of Bologna, 48121 Ravenna, Italy
[e] Consejo Superior de Investigaciones Científicas (CSIC), Museo Nacional de Ciencias Naturales, Departamento de Paleobiología, Madrid, Spain
[f] Departament d'Història i Història de l'Art, Universitat Rovira i Virgili, Avinguda de Catalunya 35, 43002, Tarragona, Spain
[g] Institut Català de Paleoecologia Humana i Evolució Social (IPHES-CERCA), Zona Educacional 4, Campus Sescelades URV (Edifici W3), 43007, Tarragona, Spain
[h] Centro Nacional de Investigación sobre la Evolución Humana (CENIEH), Paseo Sierra de Atapuerca 3, 09002 Burgos, Spain
[i] Stone Age Institute, 1392 W Dittemore Rd, Gosport, IN 47433, USA
[j] Anthropology Department, Indiana University, Bloomington, IN, USA
[k] Institute of Geosciences, Goethe University Frankfurt, 60438 Frankfurt, Germany

ARTICLE INFO

Editor: S. Dai

Keywords:
Stable strontium isotopes
Tooth enamel
Trophic niche
Grazers
Browsers

ABSTRACT

Reconstructing the trophic (paleo)ecology and associated physiological traits of both extinct and extant taxa is essential for understanding the functioning of (past) ecosystems. In this context, novel metal stable isotope proxies offer promising tools for investigating ancient diets and, to some extent, the digestive adaptations of animals. In this study, we analyzed the stable strontium isotope composition ($\delta^{88}Sr$), alongside $\delta^{13}C$, $\delta^{18}O$, and $^{87}Sr/^{86}Sr$ ratios, in fossil dental remains of herbivorous mammals from the Early Pleistocene site of Tighennif, Algeria (~1.2–1.0 Ma). Traditional carbon and oxygen isotope data indicate an environment dominated by C_3 vegetation, while the $^{87}Sr/^{86}Sr$ ratios suggest either a relatively homogeneous strontium baseline or limited geographic mobility of the animals. Our results demonstrate that $\delta^{88}Sr$ is sensitive to diagenetic alteration, with enamel samples retaining biogenic signatures comparable to those of modern mammals, whereas dentine exhibits $\delta^{88}Sr$ values shifted toward positive geogenic end-members. $\delta^{88}Sr$ patterns may reflect trophic niche differentiation among herbivores and potentially indicate distinct digestive physiologies, offering a novel alternative proxy for dietary and ecological reconstructions in the fossil record.

1. Introduction

Understanding how ancient ecosystems functioned requires detailed insights into the diets, behaviors, and ecological roles of extinct organisms. Among herbivorous taxa, even subtle differences in foraging strategies and habitat preferences can influence patterns of resource competition and ultimately shape community composition and structure (Carscadden et al., 2020). In recent years, advancements in geochemical methods have provided new avenues for reconstructing such aspects of paleoecology. Notably, the analysis of both radiogenic and stable strontium isotopes in fossil dental enamel has emerged as a powerful approach for inferring mobility, habitat use, and dietary preferences in extinct and extant taxa (Knudson et al., 2010; Guiserix et al., 2024; Griffith et al., 2025; Michailow et al., 2025; Weber et al., 2025).

Strontium (Sr) substitutes for calcium (Ca) in the hydroxyapatite of bones and teeth (Nielsen, 2004), preserving the isotopic signature of ingested food and water (see Bentley, 2006 for a review). The radiogenic strontium isotope ratio ($^{87}Sr/^{86}Sr$) reflects indeed the geological substrates of the environment animals inhabited and foraged in, thereby offering a geospatial signal that complements traditional stable isotope proxies such as $\delta^{13}C$ and $\delta^{18}O$ (see the review in Müller et al., 2024). This allows researchers to trace the movement of individuals across

* Corresponding author at: MeGic Lab, Department of Chemical and Geological Sciences, University of Modena and Reggio Emilia, Via G. Campi 103, 41125 Modena, Italy.
E-mail address: federico.lugli@unimore.it (F. Lugli).

https://doi.org/10.1016/j.palaeo.2025.113226
Received 26 May 2025; Received in revised form 22 August 2025; Accepted 22 August 2025
Available online 23 August 2025

distinct geological zones and to infer residency or migration patterns in both modern and fossil faunas (e.g., Pellegrini et al., 2008; Britton et al., 2009; Radloff et al., 2010; Copeland et al., 2016; Lugli et al., 2017; Wooller et al., 2021; Koutamanis et al., 2023; Armaroli et al., 2024).

However, this geologically-driven signal represents only part of the isotopic record. Increasing attention has been given to the stable isotopes of strontium, particularly $^{88}Sr/^{86}Sr$ (reported as $\delta^{88}Sr$ in ‰ against NIST987), representing mass-dependent fractionation between isotopes during biological and geochemical processes (Wu et al., 2024). Studies showed that lighter metal isotopes (e.g., ^{86}Sr) are preferentially incorporated into bioapatite relative to heavier ones (e.g., ^{88}Sr), a phenomenon with important implications for interpreting dietary habits and physiological adaptations among taxa (Knudson et al., 2010). Akin to calcium isotope systematics, the mechanisms driving $\delta^{88}Sr$ variability in biological tissues are not yet fully understood, and it remains unclear to what extent dietary, metabolic, or digestive physiological factors influence these values in herbivores.

In this study, we analyze fossil dental enamel from multiple herbivore families, recovered at the Early Pleistocene archaeological site of Tighennif (Algeria, ~1.2–1.0 Ma). Our goal is to reconstruct aspects of the paleoecology of these herbivores using a multi-isotope approach, with a particular focus on $\delta^{88}Sr$, an emerging proxy that holds potential for distinguishing trophic niches and digestive physiology of sympatric herbivores. Specifically, we measured first the classical isotopic systematics of $\delta^{13}C$ and $\delta^{18}O$ to assess the habitat and the occupied trophic niche, $^{87}Sr/^{86}Sr$ to evaluate provenance and landscape use, and finally $\delta^{88}Sr$ to explore potential differences in Sr isotope fractionation across taxa. In particular, we investigate whether $\delta^{88}Sr$ values vary systematically according to diet and/or digestive physiology, by comparing animals categorized as monogastric versus polygastric herbivores. This approach aims to test whether differences in digestive system anatomy and physiology may influence Sr isotope incorporation and thus reflect rooted ecological or physiological variability among extinct herbivore communities.

1.1. Premises on C-O-Sr isotope composition of bioapatite

Carbon isotope analysis of the carbonate moiety of dental enamel hydroxyapatite is a powerful tool for distinguishing between consumers of C_3 and C_4 plants. This distinction arises from the contrasting $\delta^{13}C$ signatures associated with C_3 and C_4 photosynthetic pathways (O'Leary, 1981), which are passed on to herbivores through their diet. C_3 plants – including most trees, shrubs, and cool-season grasses – typically exhibit more negative $\delta^{13}C$ values (around −30 ‰ to −22 ‰), whereas C_4 plants – mainly warm-season tropical grasses and sedges – have higher $\delta^{13}C$ values (around −14 ‰ to −10 ‰) (Cerling et al., 1997). These isotopic signals are incorporated into the herbivore enamel via the diet, with a relatively well-characterized enrichment factor of ~12–14 ‰ (Cerling et al., 1997). As enamel mineralizes during tooth development, it registers the isotopic signal of the diet during that period, enabling reconstructions of dietary preferences and infer habitat use over time. In African environments, $\delta^{13}C$ is traditionally used to classify herbivores as C_3-browsers, C_4-grazers or mixed-feeders (Cerling et al., 2015).

Oxygen isotopes in mammal enamel are in equilibrium with blood bicarbonate and are mainly controlled by the $\delta^{18}O$ composition of body water (Pederzani and Britton, 2019). This latter is, in turn, governed by the mass balance and isotopic fractionation of oxygen as it enters and exits the body. Oxygen is introduced through ingested water, inhaled O_2, and diet. Internally, metabolic processes generate H_2O and CO_2 as byproducts. Oxygen is lost via excretions – such as urine, sweat, and feces – as well as through water vapor and CO_2 in exhaled air. Under steady-state conditions, a predictable relationship exists between ingested water and body water $\delta^{18}O$ values (Luz et al., 1984). Herbivores obtain ingested water primarily from two sources: drinking water and the water contained in plants (Pederzani and Britton, 2019). While the $\delta^{18}O$ value of drinking water reflects that of meteoric precipitation, which itself is correlated with mean annual temperature (D'Angela and Longinelli, 1990), plant water is typically enriched in ^{18}O relative to groundwater due to isotope fractionation during evapotranspiration. This, in turn, suggests that herbivore's behavioral ecology may also impact the $\delta^{18}O$ value of their tissues. For example, obligate drinkers tend to exhibit lower $\delta^{18}O$ values in their tissues compared to non-obligate drinkers (see e.g. Levin et al., 2006).

The $^{87}Sr/^{86}Sr$ ratio is a well-known geochemical tracer used to investigate the geographic origin and mobility of organisms, rooted in the field of human paleoecology (Ericson, 1985). This isotopic ratio reflects the local geology because radiogenic ^{87}Sr is produced by the radioactive decay of ^{87}Rb, while ^{86}Sr is stable. Since both Sr and Rb are ubiquitously present as trace elements within the Earth's crust, crustal rocks and mantle-derived materials acquire different $^{87}Sr/^{86}Sr$ ratios in relation to their age and to their initial Sr—Rb contents. As strontium ions enter ecosystems through weathering and are taken up by plants and animals, the $^{87}Sr/^{86}Sr$ signature of a geological region becomes imprinted in biological tissues, particularly into the bioapatite of teeth and bones (Faure and Mensing, 2005). By comparing the $^{87}Sr/^{86}Sr$ values of vertebrate bioapatite with local geological baselines (e.g. Armaroli et al., 2024), one can assess whether an organism was local to a given place or originated from a different area. This approach is especially powerful in paleoecology for reconstructing patterns of animal migration and habitat use (e.g., Balter et al., 2008; Lugli et al., 2017; Wooller et al., 2021; Kowalik et al., 2023). Although fractionation along the trophic chain is expected, any eventual isotope effect is corrected during mass spectrometry analyses, due to mass bias normalization against a constant $^{88}Sr/^{86}Sr$ ratio.

Yet, this latter is known to be variable in the environment. By analysing this ratio ($\delta^{88}Sr$), using external mass bias correction (e.g. through double-spike or Zr-doping), it is possible to explore Sr isotope fractionation across different reservoirs and trophic niches (Knudson et al., 2010; Hajj et al., 2017). $\delta^{88}Sr$ can thus provide insights into physiological and dietary habits. Since Sr mainly enters the body through diet and drinking water, and is mostly extracted via the kidneys, only a small portion (10–30 %) is absorbed in the small intestine of monogastric mammals (and both small intestine and rumen for ruminants; Hyde et al., 2019), through mechanisms that passively follow Ca^{2+} metabolism. This generates an overall decrease of Sr/Ca ratios along the trophic chain (Burton et al., 1999). Most of the absorbed Sr is deposited in bone bioapatite, where lighter isotopes are preferentially fixed over heavier ones, thus resulting in a $\delta^{88}Sr$ lighter than that of the diet. This was confirmed experimentally with controlled-feeding studies, showing a $\delta^{88}Sr$ trophic shift of about −0.20 ‰ (Lewis et al., 2017; Weber et al., 2025). Still, the exact mechanisms that produce the observed isotope variability among humans and animals (see e.g. Knudson et al., 2010) remain incompletely understood. Similar isotope effects are observed for calcium (Skulan and DePaolo, 1999; Reynard et al., 2010; Heuser et al., 2011; Martin et al., 2018). The $\delta^{44/42}Ca$ values have been shown to vary between grazer and browser herbivores in modern trophic chains, suggesting that isotope differences in consumed plant tissues are retained in consumer tissues (Martin et al., 2018). Notably, other physiological mechanisms – such as e.g. digestive system features – are often invoked to explain element partitioning (Balter and Simon, 2006) and isotope ratio fractionation (Martin et al., 2018), but yet relatively unexplored.

1.2. Geoarcheological setting

The hominin site of Tighennif was discovered in 1872 during sand quarry exploitation. Subsequent explorations of the site unearthed further fossils (Balout, 1955). Large scale excavations conducted in the 1950s have led to the discovery of the oldest *Homo erectus* fossil remains in North Africa named *Atlanthropus mauritanicus*, associated with large and small mammal fossils and Acheulian stone tools (Arambourg and Hoffstetter, 1963). Tighennif is located on the High Plateaus of northwestern Algeria (35° 24′57.30" N; 0° 19′21.30″ E) in the province of

Mascara (Fig. 1). The site is formed near the northern edge of the plain of Ghriss. The plain of Ghriss consists of a depression that extends from north-east to south-west between the Jurassic Mountains of Saida in the south, which have undergone intense tectonic activities, and the Beni Chougrane folded mountains in the north of Cretaceous-Tertiary age. The sedimentary deposits around Tighennif include clays, sandy clays, sands, and sandstones dated to Miocene, Pliocene and Quaternary (Bekkoussa et al., 2008, 2013) (Fig. 1).

New multidisciplinary studies involving stratigraphy, dating, and archaeological excavations are conducted at four loci (namely A, B, D, and E) within the Tighennif site. Our work focuses on Locus A that showed a great abundance of archaeological and fossil remains. The predominantly sandy stratigraphic sequence at this locus is of fluvial origin or associated with floodplain environments. It includes three major sedimentary deposits: 1) varicolored clays with patches and $CaCO_3$ nodules; 2) in erosive discordance, a thick deposit of sand, resting on the varicolored clays, includes three parts of stratigraphic layers: lower, middle and upper. The lower part includes a layer of sandy gray clay containing stone tools and fossil bones, a deposit of fine and medium sands with carbonate clasts, and a layer of medium-size sands with clay. The middle layers, rich in archaeological remains, are sandy of medium to fine particles and mostly massive with very low clay content and $CaCO_3$ nodules. The upper layers consist of fine and very fine sands with oxidation lines; and 3) the top of the section entails a thick layer of sandstones of fine to medium sands resting on a disconformity. A caliche soil seals the stratigraphic sequence. As of the dating, comprehensive studies of clays and quartz-rich samples are underway involving paleomagnetism, Electron Spin Resonance (ESR), Optically Stimulated Luminescence (OSL), and cosmogenic nuclide ^{10}Be and ^{26}Al dating techniques. Based on faunal taxa of biostratigraphic interest, Locus A is estimated to ~1.2–1.0 Ma in age (Sahnouni and van der Made, 2009).

The lithic industry is typical of Acheulian tradition. In addition to Oldowan-type of artifacts, it is characterized primarily by the presence of Large Cutting Tools (LCT) (trihedrons, bifaces, and cleavers). It includes cores, LCTs, whole flakes, retouched pieces, various fragments, hammerstones, and unmodified cobbles. In terms of raw materials, the stone artifacts are made of sandstone, flint, quartzite, and limestone.

Taphonomic evidence clearly shows a causal association between the fossil bones and the stone artifacts. Bone surface preservation is generally good, allowing the recognition of anthropogenic modifications. The Tighennif Locus A archaeofauna record includes several bones with cut marks evidence (Chelli Cheheb, 2018). These are slicing marks occurring primarily on appendicular and axial bone elements. The majority of the cut marks are found on the lower limbs, followed by intermediate limbs and upper limbs. The activities involved in hominin butchery processes include skinning, defleshing, and evisceration. In addition, hammerstone percussed bones are documented in the form of conchoidal percussion scars, notches and impact flakes, mainly of large and very large animals suggesting intentional bone marrow extraction.

2. Materials and methods

Fossil herbivore teeth were sampled from the Locus A faunal assemblage (Saidani, 2023) of the Early Pleistocene archeological site of Tighennif (Algeria). Sampled families include: Bovidae (*Parmularius ambiguous*, *Tragelaphus algericus*, *Connochaetes taurinus progun*), Camelidae (*Camelus thomasi*), Elephantidae (*Loxodonta atlantica*), Equidae (*Equus mauritanicus*), Hippopotamidae (*Hippopotamus sirensis*), Rhinocerotidae (*Ceratotherium mauritanicum*), and Suidae (*Metridiochoerus compactus*) (Suppl. Table 1).

Enamel powder (ca. 10 mg) was drilled from $n = 49$ fossil dental specimens, along the full length of the crown. In addition, $n = 7$ dentine specimens (one sample per family) were collected as well to test the Sr isotope composition of a tissue easily altered diagenetically.

δ^{13}C and δ^{18}O isotope analyses were performed on the carbonate moiety of tooth enamel ($n = 46$) at the Centro Interdipartimentale Grandi Strumenti of the University of Modena and Reggio Emilia. Sample powders (2 mg) were reacted for 2 h at 50 °C with +100 % phosphoric acid. Isotope ratios were determined on liberated CO_2 by continuous flow IRMS (Elementar precisION) coupled to an equilibration system (Elementar isoFLOW). Repeated analyses of NBS18 and NBS19 reference materials showed a precision (1SD) of ±0.1 ‰ for δ^{13}C and ± 0.2 ‰ for δ^{18}O. C—O data are expressed in ‰ against VPDB.

Sr isotope analysis was performed at the MeGic Lab of the Department of Chemical and Geological Sciences (University of Modena and Reggio Emilia). Samples (n = 49 enamel + n = 7 dentine) were cleaned with MilliQ in an ultrasonic bath and digested with concentrated nitric acid. After Sr purification (Argentino et al., 2021), samples were diluted to 4 % vol. nitric acid and measured with the Neptune MC-ICPMS housed at the Centro Interdipartimentale Grandi Strumenti of the University of Modena and Reggio Emilia. δ^{88}Sr and ^{87}Sr/^{86}Sr were collected simultaneously following Argentino et al. (2021). Data were reported to a NIST SRM 987 value of 0.710248 (McArthur et al., 2001). Repeated analysis of SRM 987 yielded an average ^{87}Sr/^{86}Sr of 0.710251 ± 0.000016 (2SD, $n = 21$) and a reproducibility of ±0.05 ‰ (1SD, n = 21) for δ^{88}Sr. A NIST SRM 1400 (Bone Ash) processed along with the samples yielded an ^{87}Sr/^{86}Sr ratio of 0.71310 ± 0.00001 (2SE) and a δ^{88}Sr of −0.37 ‰ ± 0.02 (2SE), in agreement with literature data (Romaniello et al., 2015; Guiserix et al., 2022; Weber et al., 2018, 2025). δ^{88}Sr data are expressed in ‰ against NIST RMS 987. All data generated during this study are included in this manuscript and its supplementary materials.

Statistical analyses were conducted in R (version 4.0.5). Individual samples were analyzed after grouping by taxonomic family and digestive system type (monogastric vs. polygastric). Among polygastric

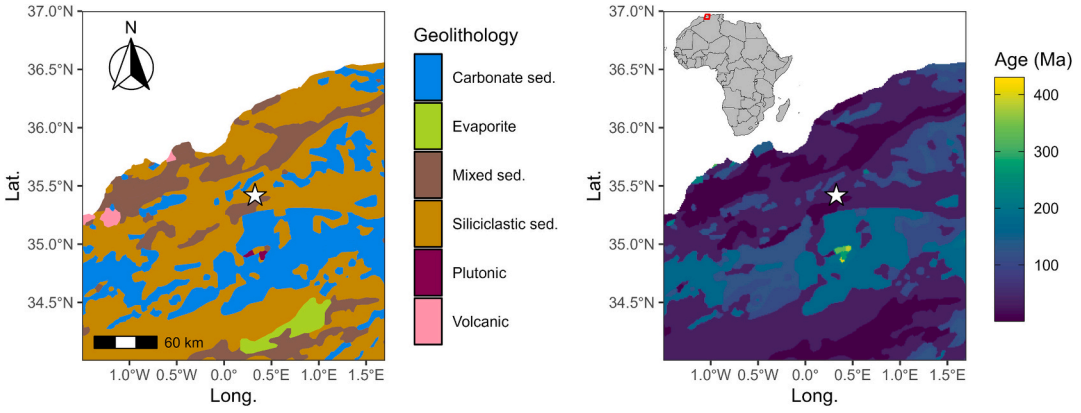

Fig. 1. Geolithological map from GLiM (Hartmann and Moosdorf, 2012) of the area surrounding Tigheniff (white star). The age of the rocks from GLiM is also reported.

animals, we included both true ruminants (Bovidae, four-chambered stomach) and non-ruminant foregut fermenters with a three-chambered stomach, such as Camelidae (Niehaus and Mora, 2022) and Hippopotamidae (Clauss et al., 2004). Due to the small sample sizes of some families and the lack of homogeneity of variances, normality assumptions could not be met. Therefore, differences among groups were assessed using the non-parametric Kruskal-Wallis test. Post hoc pairwise comparisons were performed using Dunn's test with Holm correction for multiple testing. Isotopic differences between monogastric and polygastric groups were evaluated using the Wilcoxon rank-sum test, while paired Wilcoxon rank-sum tests were applied to compare dentine-enamel pairs. Statistical significance was set at $p < 0.05$.

3. Results

Our dataset is composed of four isotope ratios, namely $\delta^{13}C_{VPDB}$, $\delta^{18}O_{VPDB}$, $\delta^{88}Sr_{NIST987}$ and $^{87}Sr/^{86}Sr$ measured on tooth enamel (Suppl. Table 1). $\delta^{88}Sr$ and $^{87}Sr/^{86}Sr$ were measured on a subset of dentine samples, to help interpret the diagenetic pathways of Sr in teeth. Enamel $\delta^{13}C_{VPDB}$ showed an average value of −10.2 ‰ ± 0.93 ‰ (1SD, $n = 46$), ranging between −11.7 ‰ and − 7.3 ‰; while $\delta^{18}O$ showed an average value of −3.6 ‰ ± 1.1 ‰ (1SD, n = 46), ranging between −6.4 ‰ and − 2.0 ‰ (Fig. 2). $\delta^{88}Sr$ showed an average value of −0.28 ‰ ± 0.11 ‰ (1SD, $n = 49$, min = −0.53 ‰, max = −0.10 ‰) for enamel and − 0.05 ‰ ± 0.07 ‰ (1SD, $n = 7$, min = −0.19 ‰, max = 0.02 ‰) for dentine specimens (Fig. 3). $^{87}Sr/^{86}Sr$ showed an average value of 0.70918 ± 0.00013 (1SD, n = 49, min = 0.70893, max = 0.70950) for enamel and 0.70916 ± 0.00010 (1SD, n = 7, min = 0.70897, max = 0.70930) for dentine specimens (Fig. 3). For each tooth where both dentine and enamel were measured, a difference ($\Delta_{dentine\text{-}enamel}$) between the two tissues was calculated. The average $\Delta_{dentine\text{-}enamel}$ values are 0.24 ‰ ± 0.11 ‰ (1SD, n = 7) for $\delta^{88}Sr$ and 0.00003 ± 0.00007 (1SD, n = 7) for $^{87}Sr/^{86}Sr$. The difference between the enamel and dentine datasets was evaluated with a paired Wilcoxon rank sum test, resulting in a significant difference for $\delta^{88}Sr$ ($p = 0.016$), but not for $^{87}Sr/^{86}Sr$ ($p = 0.22$). Summary statistics for each taxonomic family group are reported in Table 1.

The non-parametric Kruskal-Wallis test was used to compare the data among families. The test showed statistically significant differences for $\delta^{88}Sr$ and $\delta^{18}O$ ratios ($p = 8e\text{-}04$, $p = 0.001$ respectively), but not for $^{87}Sr/^{86}Sr$ and $\delta^{13}C$ ($p = 0.54$, $p = 0.37$ respectively). $\delta^{88}Sr$ and $\delta^{18}O$ post hoc Dunn tests are reported in Table 2 for family-pairs. When grouped by digestive system, both $\delta^{88}Sr$ and $^{87}Sr/^{86}Sr$ ratios differed significantly between monogastric (hindgut fermenters) and polygastric (foregut fermenters) vertebrates (Wilcoxon rank sum test, $p = 2.5e\text{-}05$ and $p = 0.04$ respectively), whereas no significant differences were observed for $\delta^{13}C$ or $\delta^{18}O$ ($p = 0.62$ and $p = 0.11$ respectively). It should be noted that, due to the low number of individuals in some families, much of the observed variance is likely driven by Equidae and Bovidae. Caution is therefore warranted when interpreting patterns for families represented by few specimens.

4. Discussion

4.1. Diagenetic alteration of Sr in bioapatite: inferences from the $\delta^{88}Sr$ ratio

Understanding the diagenetic alteration of Sr in fossil bioapatite dental and bone specimens is key to unravel the origin of the observed isotope signal, i.e. if it is of post-depositional or biogenic origin. Enamel is nowadays considered a robust proxy for metal isotope analyses, due to its intrinsic resistance to diagenetic alteration, driven by its compact and low-organic structure. Yet, especially for deep-time, Sr isotope signals can be found altered by post-depositional uptake of Sr (see e.g. Michailow et al., 2025).

Many proxies are currently used for diagenetic assessment of

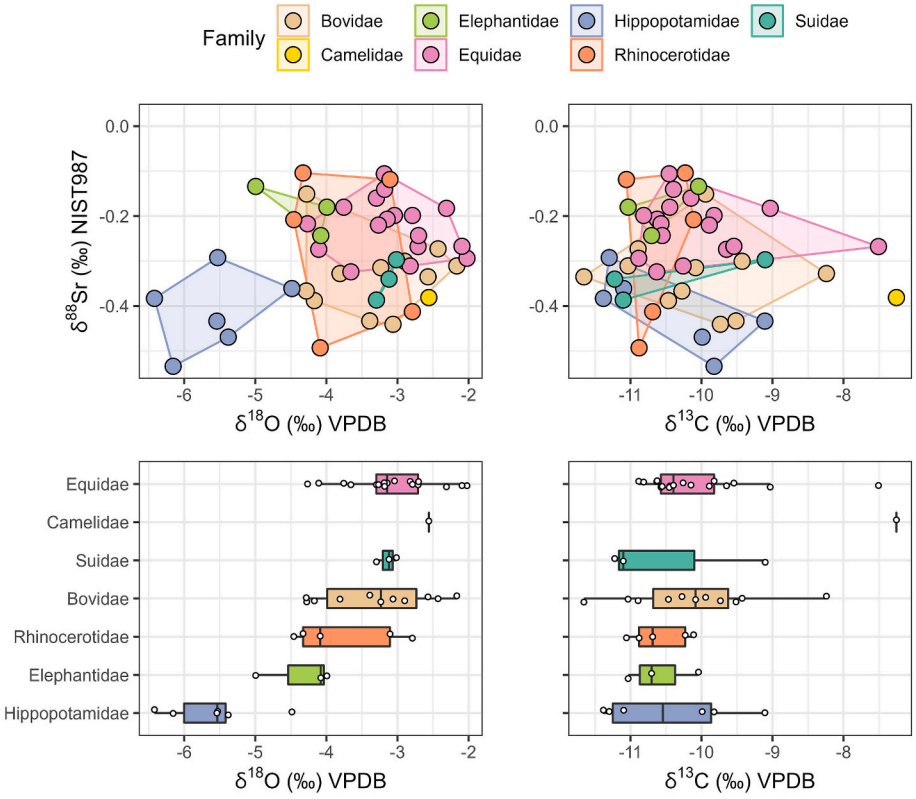

Fig. 2. $\delta^{88}Sr$ data are compared with $\delta^{18}O$ and $\delta^{13}C$ for the different families. Boxplots represent data distribution of individual families; these are reordered based on the family $\delta^{18}O$ average value.

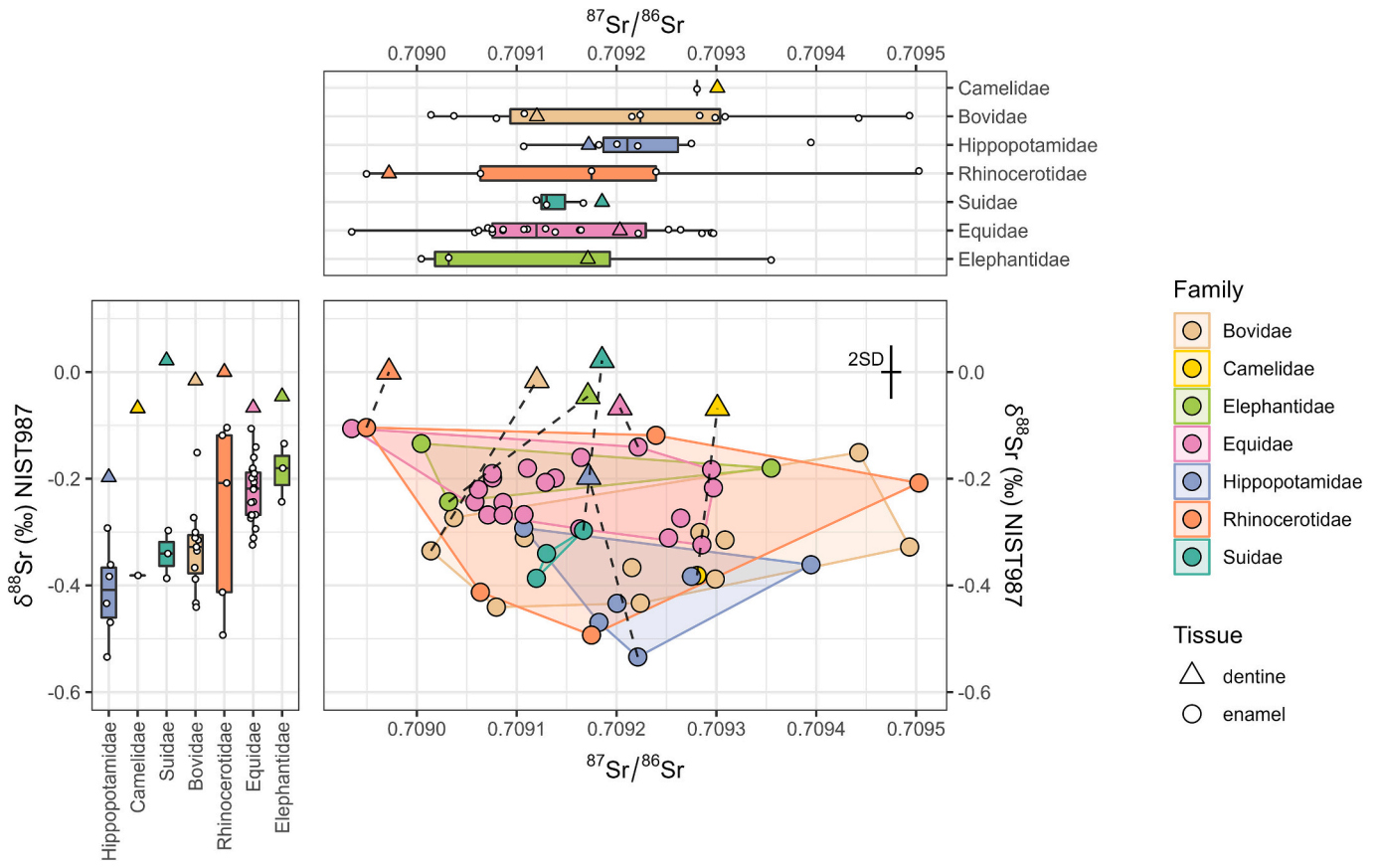

Fig. 3. Enamel (circles) and dentine (triangles) Sr isotope data ($\delta^{88}Sr$ and $^{87}Sr/^{86}Sr$) of herbivores at Tighennif. In the main panel, dashed lines connect dentine-enamel pairs (i.e., sampled from the same tooth). 2SD is 0.1‰ for $\delta^{88}Sr$ and 0.00002 for $^{87}Sr/^{86}Sr$. In the side graphs, boxplots represent data distribution of individual families; these are reordered based on the family average isotope value.

vertebrate bioapatite (e.g. spectroscopic, immunochemical or elemental data; see Thomas et al., 2011; France et al., 2014; Lugli et al., 2021; Gatti et al., 2022; Simpson et al., 2023; Del Valle et al., 2025) but, although robust, their relation with the Sr composition of a sample is not always straightforward nor easy to interpret. Michailow et al. (2025) proposed the use of $\delta^{88}Sr$ ratio itself as a proxy for the overall Sr isotope composition preservation in terrestrial vertebrate bioapatite. This is based on the fact that biogenic apatite values tend to be lower than 0 ‰ (terrestrial vertebrate bioapatite ~ −0.20 ‰ on average, Knudson et al., 2010), while geogenic (diagenetic) end-members are commonly higher than 0 ‰ (e.g., soils: from 0.02 ‰ to 0.37 ‰, seawater: ~ 0.39 ‰, continental crust average: ~ 0.30 ‰, modern continental carbonates: from 0.00 ‰ to 0.38 ‰; Wu et al., 2024).

A trend toward more positive values can be observed in our data for dentine samples, retaining a more positive $\delta^{88}Sr$ signature (−0.05 ‰ on average) than enamel samples (−0.28 ‰ on average), and an average difference of 0.23 ‰ (Fig. 4). Additionally, paired dentine-enamel specimens show a statistically significant difference ($p = 0.016$). A similar – though smaller – difference was observed in Late Pleistocene samples from France (Guiserix et al., 2024), where bone data were significantly higher than enamel (Wilcoxon rank sum $p = 0.002$), with an average bone-enamel difference of ~0.1 ‰. Notably, the overall $\Delta^{88}Sr_{bone-tooth}$ found in modern reptiles is 0.11 ‰ ± 0.04 ‰ (Weber et al., 2025). This value can be used as a conservative preliminary threshold to discriminate between physiological and diagenetic offsets between bone and tooth specimens.

Overall, these observations indicate that the $\delta^{88}Sr$ in our enamel samples are largely of biological origin, showing minimal or no post-deposition alteration, whereas dentine appears to be at least partially overprinted by diagenetic uptake of (soil-derived) Sr. The good preservation of enamel data is further supported by the striking similarity between $\delta^{88}Sr$ values in our samples and those reported for bones of extant African herbivores (Tütken et al.: −0.30 ‰ ± 0.17 ‰ vs. our data: −0.28 ‰ ± 0.11 ‰, see Fig. 5). A statistically significant negative correlation between $\Delta^{88}Sr_{dentine-enamel}$ and $\delta^{88}Sr_{enamel}$ ($R^2 = 0.77$, $p = 0.01$, Fig. 6), suggests that all dentine is trending toward a local diagenetic end-member, with $\delta^{88}Sr$ value around ~0 ‰. Samples with 'more negative' biogenic values – assumed here to be represented by the enamel – tend to show a greater difference between dentine and enamel, possibly linked to a partial retaining of the original biogenic signal.

We can extend our interpretation of $\delta^{88}Sr$ data to the $^{87}Sr/^{86}Sr$ ratio. A conservative hypothesis is that if a sample's $\delta^{88}Sr$ value has been affected by diagenesis, its $^{87}Sr/^{86}Sr$ ratio is also to be considered altered (Michailow et al., 2025). This idea assumes that the $\delta^{88}Sr$ data reflect simple mixing between biogenic and diagenetic end-members, with negligible isotopic fractionation during post-depositional Sr uptake, a process that, to date, remains uncharacterized. Yet, the $^{87}Sr/^{86}Sr$ ratio shows limited variability among our (~normally-distributed) enamel samples (SD ~0.0001) (Fig. 4), consistent with findings from other studies in the area (Fannin et al., 2021), likely due to the relatively simple and homogeneous local geology. Assuming isotopically similar local bioavailable and diagenetic end-members, it remains challenging to distinguish between biogenic and diagenetic contributions to the $^{87}Sr/^{86}Sr$ signal. Indeed, no significant correlation is found between $\Delta^{87}Sr/^{86}Sr_{dentine-enamel}$ and $^{87}Sr/^{86}Sr_{enamel}$ ($R^2 = 0.39$, $p = 0.13$), nor is there a significant difference between paired dentine and enamel values ($p = 0.22$; Fig. 6). Notably, the $^{87}Sr/^{86}Sr$ standard deviation of dentine samples is 0.00010 – slightly lower than the SD of respective enamel specimens (0.00013) – which may suggest an (expected) homogenization due to diagenetic alteration.

Table 1
Summary statistics for enamel isotope data; Sr isotope dentine values are reported as well (1 sample measured for each family).

	$\delta^{88}Sr_{NIST987}$ (‰)						$^{87}Sr/^{86}Sr$					$\delta^{13}C_{VPDB}$ (‰)					$\delta^{18}O_{VPDB}$ (‰)				
Family	Mean	SD	Max	Min	n	Dentine	Mean	SD	Max	Min	n	Dentine	Mean	SD	Max	Min	n	Mean	SD	Max	Min	n
Bovidae	−0.33	0.08	−0.15	−0.44	11	−0.02	0.70923	0.00016	0.70949	0.70901	11	0.70912	−10.1	0.9	−8.2	−11.7	11	−3.3	0.8	−2.2	−4.3	11
Camelidae	−0.38	NA	NA	NA	1	−0.07	0.70928	NA	0.70928	0.70928	1	0.70930	−7.3	NA	NA	NA	1	−2.6	NA	NA	NA	1
Elephantidae	−0.19	0.05	−0.13	−0.24	3	−0.05	0.70913	0.00019	0.70935	0.70900	3	0.70917	−10.6	0.5	−10.0	−11.0	3	−4.4	0.6	−4.0	−5.0	3
Equidae	−0.22	0.06	−0.11	−0.32	20	−0.07	0.70914	0.00010	0.70930	0.70893	20	0.70920	−10.1	0.8	−7.5	−10.9	17	−3.1	0.6	−2.0	−4.3	17
Hippopotamidae	−0.41	0.09	−0.29	−0.53	6	−0.20	0.70923	0.00010	0.70939	0.70911	6	0.70917	−10.4	0.9	−9.1	−11.4	6	−5.6	0.7	−4.5	−6.4	6
Rhinocerotidae	−0.27	0.18	−0.10	−0.49	5	0.00	0.70919	0.00021	0.70950	0.70895	5	0.70917	−10.6	0.4	−10.1	−11.1	5	−3.8	0.8	−2.8	−4.5	5
Suidae	−0.34	0.04	−0.30	−0.39	3	0.02	0.70914	0.00002	0.70917	0.70912	3	0.70919	−10.5	1.2	−9.1	−11.2	3	−3.1	0.1	−3.0	−3.3	3

4.2. C-O paleoecology of herbivores at Tighennif

Carbon and oxygen isotopes are commonly measured on tooth enamel carbonate moiety to infer about vertebrate past ecology. Specifically, $\delta^{13}C$ isotope analysis is exploited for African environments, commonly rich in C_4 grasses, to distinguish between browsing and grazing eating adaptations (Cerling et al., 2003). Our $\delta^{13}C$ dataset aligns with those of Bocherens et al. (1996) and Fannin et al. (2021), with almost all the animals showing ^{13}C-depleted values, typical of C_3-browsers (Fig. 2). Yet, this is true also for mammals known to be mainly grazers, as for example white rhinoceros (*Ceratotherium* sp.). $\delta^{13}C$ analyses of tooth enamel from the Turkana Basin (Cerling et al., 2015) show that taxa similar to those studied here were predominantly C_4 grazers (or at most mixed C_3–C_4 feeders) around 1 Ma. This suggests that all the families considered in this study likely fed on C_3 grasses, advocating for the near absence of C_4 biomass from the environment. Yet, we cannot fully exclude limited browsing or mixed-feeding due to the relatively homogenous $\delta^{13}C$ data. The two highest $\delta^{13}C$ values of the dataset were observed for an equid (−7.5 ‰) and a camelid (−7.3 ‰) (Fig. 2), possibly suggesting a limited intake of C_4 plants or a minimal diagenetic alteration, an effect not reflected in their $\delta^{88}Sr$ enamel values.

$\delta^{18}O$ ratios have been used to differentiate ecological behaviors among mammals, as they reflect the isotopic composition of ingested water and food through equilibrium with blood bicarbonate. In our study, $\delta^{18}O$ ratios are different among families (Kruskal-Wallis $p = 0.001$), yet the post hoc tests showed that these differences are mainly driven by the ^{18}O-depleted values of Hippopotamidae (Fig. 2). This latter taxonomic group shows indeed low $\delta^{18}O$ (−5.6 ‰ on average), as in e.g. Bocherens et al. (1996) and Cerling et al. (2008). This is commonly interpreted as their exploitation of aquatic foodstuffs, being diurnally aquatic. Other hypotheses have been put forward to explain this lowering of the $\delta^{18}O$, including the reduced transcutaneous evaporation living daily in the water or the higher proportion of ingested water compared to other mammals. Further discussion on Hippopotamidae is provided in the section about the $\delta^{88}Sr$ ratio.

4.3. $^{87}Sr/^{86}Sr$ isotope ratios and animal mobility

The radiogenic Sr isotope ratio of dental enamel is a well-known proxy used to reconstruct human and animal mobility. In our study, the $^{87}Sr/^{86}Sr$ ratio of tooth enamel is remarkably homogeneous among animal families (Kruskal-Wallis $p = 0.54$), and shows a limited variability (SD ~0.0001) (Fig. 3). Overall, the values agree with a local geology mainly composed by sedimentary sequences of limestones, sands and clays of various ages, dated between the Mesozoic and the Cenozoic, for tens of kilometers around the site (see Fig. 1). This in turn might suggest that: 1) the faunal assemblage at Tighennif site is composed by local or in general low-mobile animals or 2) that the likely homogeneity of local geology (Fig. 1) is masking the movements of the investigated individuals. The largest $^{87}Sr/^{86}Sr$ variability is shown by Rhinocerotidae, possibly indicating a larger home-range for this taxon, compared to the others.

The significant difference between the $^{87}Sr/^{86}Sr$ ratio of monogastric and polygastric mammals ($p = 0.04$) might indicate a different use of food resources in the area or a different bioavailability of Sr end-members for animals with different digestive systems (Fig. 7). Monogastric and polygastric animals differ fundamentally in their digestive physiology, which can influence both the types of plant materials they exploit and the degree to which dietary strontium is retained. Yet, it is important to note that the difference between the two groups is minimal (0.00008), with a p value close to 0.05. This suggests that the observed difference could potentially be due to chance, and interpretations should be made cautiously.

Table 2
Result of post-hoc Dunn comparison between Family-pairs; significant values for both adjusted and unadjusted tests are reported in italics.

	$\delta^{88}Sr$			$\delta^{18}O$		
Comparison	Z	*p* unadj.	*p* adj. (Holm)	Z	*p* unadj.	*p* adj. (Holm)
Bovidae - Camelidae	0.420	0.674	1.000	−1.050	0.293	1.000
Bovidae - Elephantidae	−2.406	*0.016*	0.290	1.518	0.129	1.000
Camelidae - Elephantidae	−1.737	0.082	1.000	1.807	0.071	1.000
Bovidae - Equidae	−2.969	*0.003*	0.057	−0.684	0.494	1.000
Camelidae - Equidae	−1.516	0.129	1.000	0.809	0.418	1.000
Elephantidae - Equidae	0.731	0.465	1.000	−2.001	*0.045*	0.771
Bovidae - Hippopotamidae	1.095	0.274	1.000	3.318	*0.001*	*0.018*
Camelidae - Hippopotamidae	0.108	0.914	0.914	2.575	*0.010*	0.180
Elephantidae - Hippopotamidae	3.002	*0.003*	0.054	0.983	0.325	1.000
Equidae - Hippopotamidae	3.588	*0.000*	*0.007*	4.104	*0.000*	*0.001*
Bovidae - Rhinocerotidae	−1.392	0.164	1.000	0.922	0.357	1.000
Camelidae - Rhinocerotidae	−1.086	0.277	1.000	1.455	0.146	1.000
Elephantidae - Rhinocerotidae	1.118	0.264	1.000	−0.673	0.501	1.000
Equidae - Rhinocerotidae	0.728	0.467	1.000	1.497	0.134	1.000
Hippopotamidae - Rhinocerotidae	−2.157	*0.031*	0.527	−1.960	*0.050*	0.799
Bovidae - Suidae	0.244	0.807	1.000	−0.236	0.814	1.000
Camelidae - Suidae	−0.242	0.808	1.000	0.817	0.414	1.000
Elephantidae - Suidae	2.114	*0.034*	0.552	−1.399	0.162	1.000
Equidae - Suidae	2.057	*0.040*	0.595	0.177	0.859	0.859
Hippopotamidae - Suidae	−0.561	0.575	1.000	−2.599	*0.009*	0.178
Rhinocerotidae - Suidae	1.246	0.213	1.000	−0.891	0.373	1.000

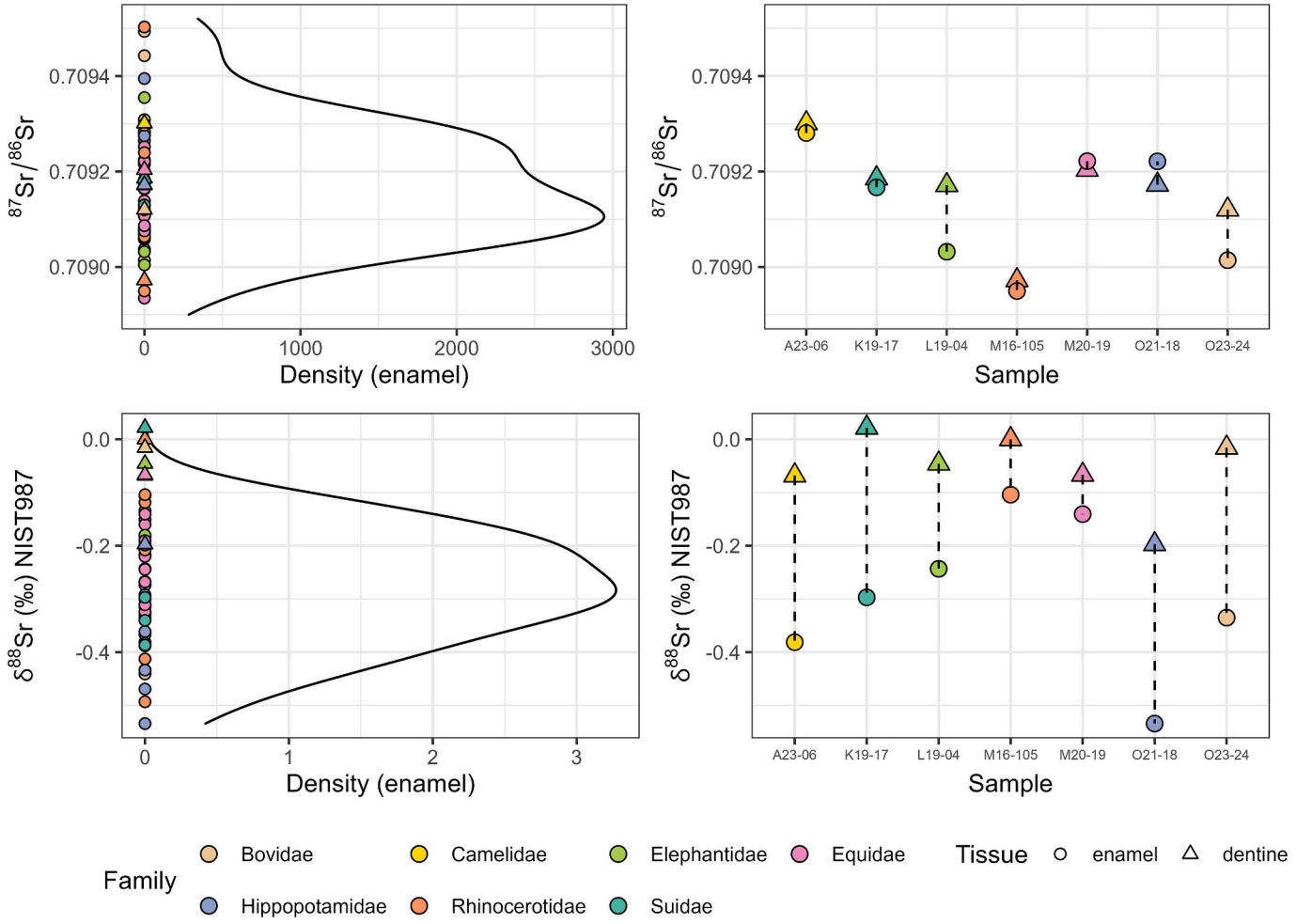

Fig. 4. (Left) Kernel-density estimations of Sr isotope data; dentine values are reported as comparison. (Right) $\delta^{88}Sr$ and $^{87}Sr/^{86}Sr$ for dentine-enamel pairs are reported for each tooth sample.

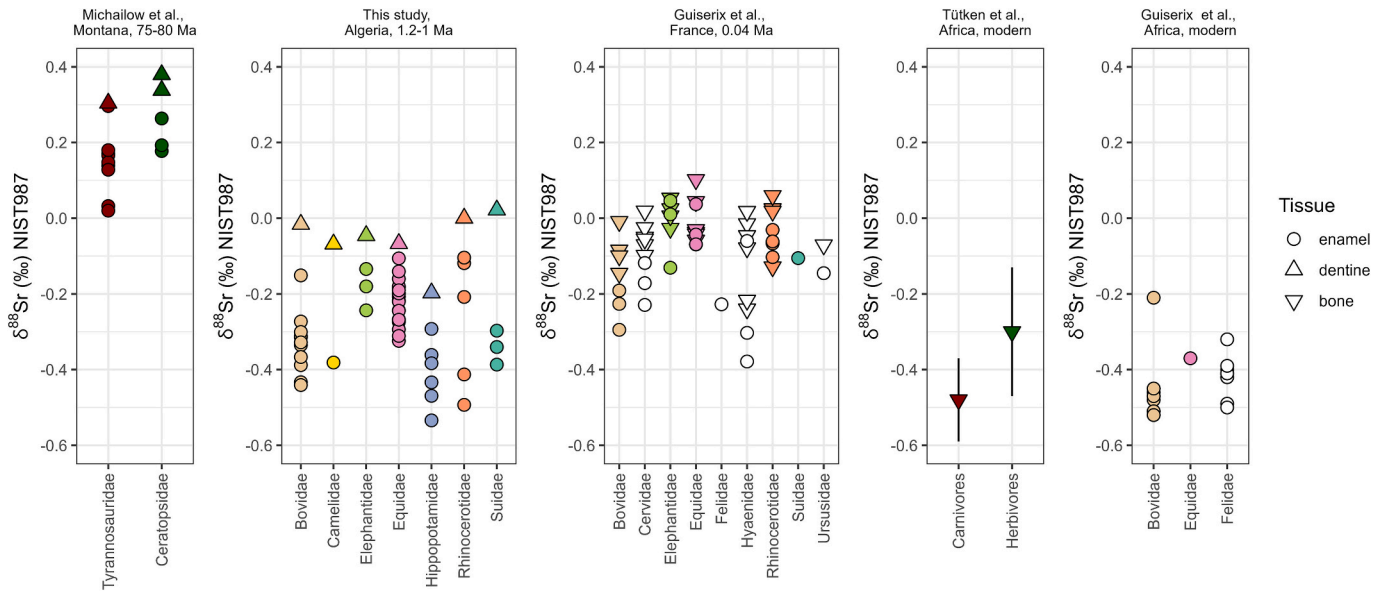

Fig. 5. $\delta^{88}Sr$ data of herbivores from Algeria (this study) are compared with bone and enamel data of vertebrates from different chronological and geographical contexts. A clear trend appears with older samples (e.g. dinosaurs) and tissues easily affected by diagenetic alteration (bone and dentine) showing the highest $\delta^{88}Sr$ values. Data are from: Michailow et al. (2025), Guiserix et al. (2024), Guiserix et al. (2022), Tütken et al. (2015).

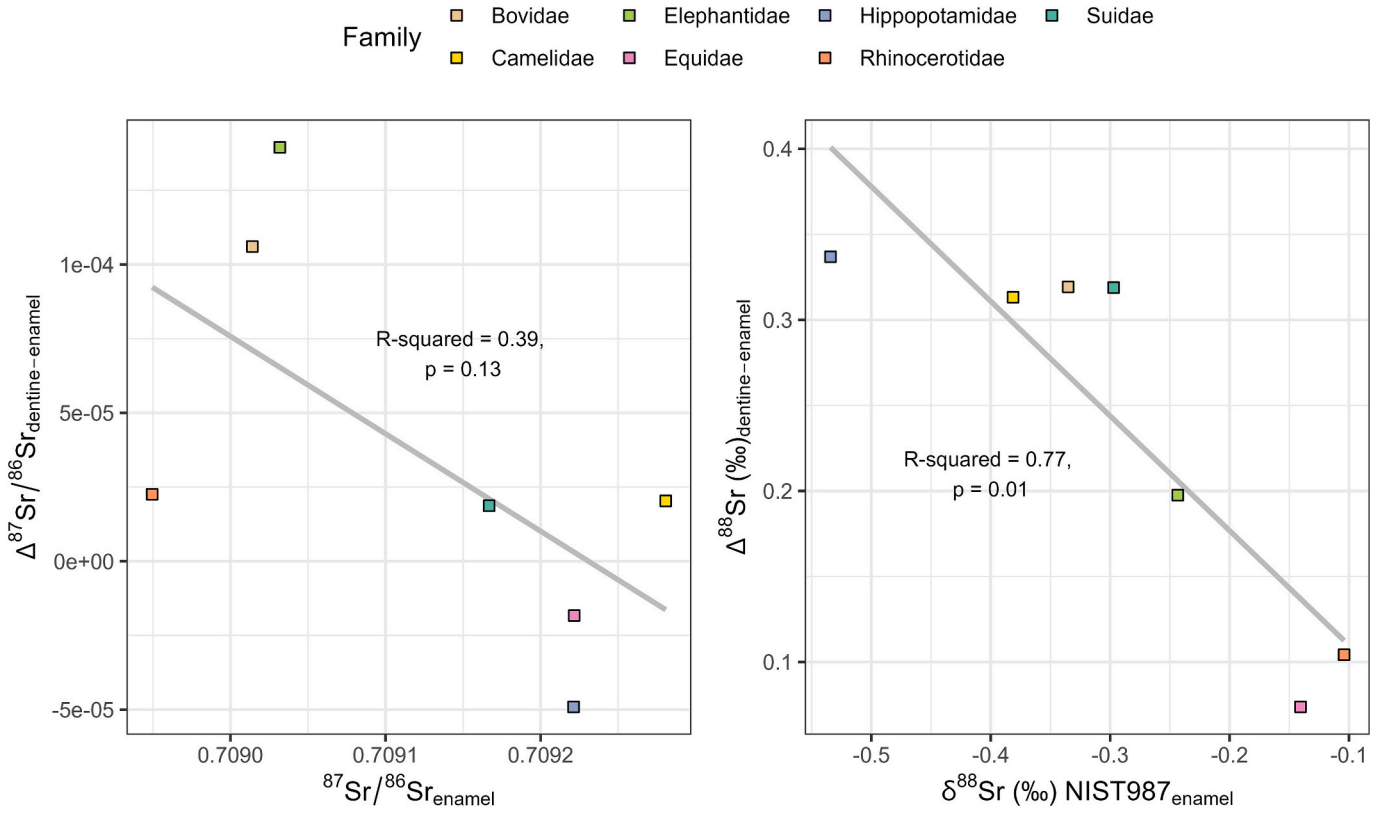

Fig. 6. $\Delta^{88}Sr_{dentine\text{-}enamel}$ and $\Delta^{87}Sr/^{86}Sr_{dentine\text{-}enamel}$ are plotted vs. $\delta^{88}Sr_{enamel}$ and $^{87}Sr/^{86}Sr_{enamel}$ respectively for each family. Gray lines are fitted linear models.

4.4. $\delta^{88}Sr$: diet and digestive system physiology

Recent works on $\delta^{88}Sr$ ratios of dental and bone tissues suggest it can be a relevant proxy for paleodiet of extant and extinct vertebrates. Specifically, it has been shown that a trophic level spacing might occur between tissues of sympatric herbivores and carnivores of ~0.20 ‰ (Weber et al., 2025). In addition, Lewis et al. (2017) reported a $\Delta^{88}Sr_{diet\text{-}tooth}$ offset of 0.32 ‰ in a controlled feeding experiment with pigs. This is generally interpreted as the preferential incorporation of light Sr isotopes in mineralized tissues (i.e. ^{88}Sr-depleted bioapatite) compared to the overall diet, similar to Ca behavior. This latter (as $\delta^{44/42}Ca$) shows a trophic level spacing of ~0.30–0.40 ‰ (Tütken et al., 2015; Martin et al., 2018), with more ^{44}Ca-depleted values at higher trophic levels.

Differences among herbivores with different trophic niches are also

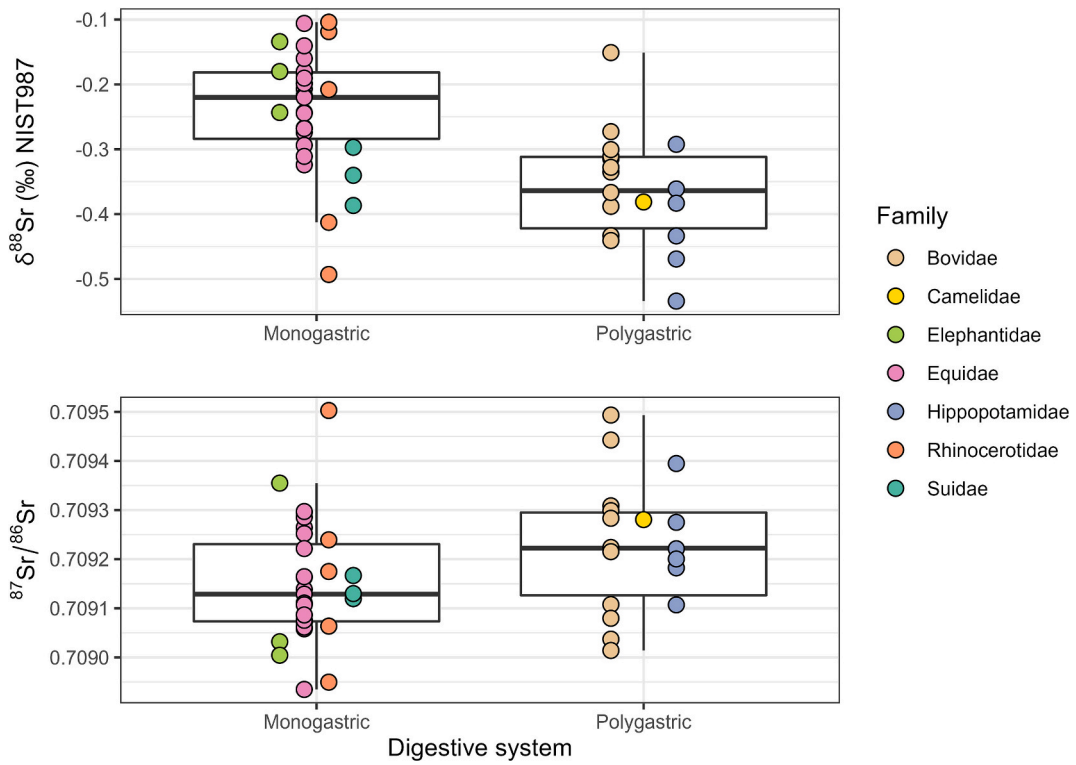

Fig. 7. Boxplots representing herbivore enamel data ($\delta^{88}Sr$ and $^{87}Sr/^{86}Sr$) clustered by digestive system physiology, namely monogastric (hindgut fermenters) vs. polygastric (foregut fermenters) animals. Both $\delta^{88}Sr$ and $^{87}Sr/^{86}Sr$ are significantly different between monogastric and polygastric herbivores (Wilcoxon rank-sum test p = 2.5e-05 and p = 0.04, respectively).

likely expected, due to the difference in stable Sr isotope compositions of plant organs. A few studies dealt with plant organs variability for $\delta^{88}Sr$. Bullen and Chadwick (2016) found the following values for a *Metrosideros polymorpha* (angiosperm) from Hawaii: roots = −0.53 ‰, stem = −0.30 ‰ and foliage = −0.12 ‰. Angiosperms and gymnosperms from Chile show differences between the individual organs ranging between 0.04 ‰ to 0.83 ‰, with median plant organ values as follow: leaf = 0.27 ‰, twig = 0.21 ‰, stem = 0.14 ‰, root = 0.01 ‰ (Oeser and von Blanckenburg, 2020). In general, $\delta^{88}Sr$ appears to increase systematically from stem and roots toward leaves.

A similar trophic niche separation (i.e., browsers vs. grazers) was observed for calcium isotopes in African herbivores (Martin et al., 2018). In our dataset, $\delta^{88}Sr$ enamel values differ significantly among mammalian families (Kruskal-Wallis p = 8e-04). However, post hoc Dunn tests with Holm correction for multiple comparisons reveal a statistically significant difference only between Equidae and Hippopotamidae. This result is likely influenced by the relatively high number of taxonomic groups compared to the limited sample size, which increases the stringency of the Holm correction and reduces the statistical power of the post hoc comparisons. In addition, we acknowledge the low number of individuals in certain families warrants caution when interpreting both the statistical tests and apparent group differences. If we observe the data, it is evident that other family-pairs show (almost) non-overlapping data ranges (see Fig. 3). A general trend can be seen, with Equidae and Elephantidae showing higher $\delta^{88}Sr$ ratios (~ − 0.20 ‰), while Alcelaphinae, Suidae and Camelidae lower (~ − 0.35 ‰) (Fig. 3). Rhinoceros and Hippopotamidae will be discussed separately due to their unique features, namely the largest isotope variability and the average lowest $\delta^{88}Sr$ ratio, respectively.

The difference between these groups (i.e., Equidae + Elephantidae vs. Alcelaphinae + Suidae + Camelidae) is approximately 0.15 ‰, slightly smaller than the expected trophic level offset but still noteworthy. Based on the literature $\delta^{88}Sr$ distribution across plant organs, this pattern may reflect a dietary preference for leafy browse among Equidae and Elephantidae, and a greater intake of grass stems, basal shoots, and potentially root tissues among Alcelaphinae, Suidae, and Camelidae. This interpretation is broadly consistent with modern African ecological patterns, where, for instance, Alcelaphinae are specialized grazers and Suidae frequently consume subterranean plant parts. Modern warthogs – phylogenetically close to *Metridiochoerus* – are known to eat grass rhizomes in the dry season.

However, while this model may partially explain the observed offset, it does not fully account for the ~0.15 ‰ difference. Notably, the average $\delta^{44/42}Ca$ difference between modern browsing and grazing herbivores is ~0.18 ‰ (Martin et al., 2018), which – given the roughly twofold lower mass-dependent fractionation of Sr relative to Ca – would predict a smaller $\delta^{88}Sr$ difference. Moreover, this model would require an almost exclusive reliance on browsing by 1 Ma African Equidae and Elephantidae, which contradicts paleoecological evidence from other studies (Cerling et al., 2015). However, the limited number of studies on $\delta^{88}Sr$ variability across plant species of different geographical areas prevents any definitive conclusions.

Rhinoceroses exhibit the highest $\delta^{88}Sr$ variability in the dataset (SD ~0.2 ‰), mirroring the pattern observed in $^{87}Sr/^{86}Sr$ values (Fig. 3). Previous intra-tooth elemental analyses of rhinoceros enamel have revealed both high variability and elevated Sr/Ca ratios compared to other herbivores (Martin et al., 2018; Kubat et al., 2023), which the authors attribute to the incidental ingestion of soil particles. An alternative explanation may lie in greater dietary plasticity – i.e., consumption of a wider variety of plants or plant parts – although modern white rhinoceroses are considered highly specialized grazers with limited dietary flexibility (Shrader et al., 2006). Additionally, if the broader $^{87}Sr/^{86}Sr$ range reflects a wider home range, it is plausible that individuals accessed multiple food and freshwater resources with potentially distinct $\delta^{88}Sr$ signatures (Andrew et al., 2016). However, the degree of isotope heterogeneity of bioavailable $\delta^{88}Sr$ across landscapes and lithologies is not yet fully known. In this regard, we found no relation between the two Sr isotope proxies – i.e., $\delta^{88}Sr$ vs. $^{87}Sr/^{86}Sr$ – in

rhinoceros ($R^2 = 0.00$, $p = 0.93$, $n = 5$), nor across the entire dataset ($R^2 = 0.02$, $p = 0.27$, $n = 49$).

The Hippopotamidae family shows the average lowest $\delta^{88}Sr$ ratios of the dataset (−0.41 ‰). Similarly, Martin et al. (2018) found Hippopotamidae to have remarkably low $\delta^{44/42}Ca$ ratios, akin to sympatric carnivores. In addition, we have seen Hippopotamidae as outliers for their ^{18}O-depleted isotope values. Others have speculated that such low-$\delta^{18}O$ ratios can be linked to the exploitation of freshwater food resources or the higher consumption of drinking water compared with other herbivores. If this were the case, we would eventually expect a shift toward higher $\delta^{88}Sr$ ratios, due to the generally higher $\delta^{88}Sr$ ratio of freshwater pools (average ~ 0.30 ‰) compared to plants and soils (Andrews et al., 2016; Nitzsche et al., 2022). Additional data are needed to fully resolve these potential mixings. Martin et al. (2018) further proposed that the low $\delta^{44/42}Ca$ ratios observed in hippos could result from physiological adaptations to a semi-aquatic lifestyle, such as increased bone density (Wall, 1983) or other skeletal modifications affecting isotope fractionation. Given that strontium follows similar metabolic and skeletal pathways as calcium, these physiological effects could plausibly contribute to the observed low $\delta^{88}Sr$ ratios. Thus, the distinctive isotopic signatures of Hippopotamidae may reflect a combination of ecological, dietary, and physiological factors, underscoring the need for integrated multi-isotope studies to fully interpret their geochemical signals.

Our data seem to suggest that diet itself cannot fully explain alone the observed variability among families. We thus consider alternative hypotheses. The observed difference (Wilcoxon rank-sum $p = 2.5e\text{-}05$) in $\delta^{88}Sr$ ratios between monogastric (i.e. hindgut fermenters: Elephantidae, Equidae, Rhinocerotidae and Suidae) and polygastric (i.e. foregut fermenters: Bovidae, Camelidae and Hippopotamidae) herbivores can possibly reflect differences in strontium absorption and fractionation during digestion and metabolism, which are influenced by their distinct digestive physiologies – but note that Suidae, though monogastric, would better fit datawise the polygastric cluster (Fig. 7). Guiserix et al. (2022) found relatively low-$\delta^{88}Sr$ values (~ −0.45 ‰) for modern herbivore enamel samples at two South Africa sites (Kruger National Park and Western Cape), slightly lower (~ −0.42 ‰) than local carnivores; yet, the majority of the sample considered were Bovidae (i.e. polygastric, mean $\delta^{88}Sr$ = −0.48 ‰). The highest $\delta^{88}Sr$ values of the Guiserix et al. (2022) dataset were observed for an *Equus burchellii* (monogastric Equidae, −0.37 ‰) and for a *Sylvicapra grimmia* (polygastric Bovidae, −0.21 ‰). However, this latter showed a remarkably high $^{87}Sr/^{86}Sr$ ratio (~0.760) compared to other individuals, suggesting different habitats and places of origin and thus considered an outlier from the authors themselves. The $\Delta^{88}Sr$ between *Equus burchellii* and Bovidae in Guiserix et al. (2022) (*Sylvicapra grimmia* excluded) is 0.11 ‰, identical to the offset found in this study between Equidae and Bovidae group means (0.11 ‰) (Fig. 5). These results are consistent – though smaller – with the findings of Guiserix et al. (2024) where the $\Delta^{88}Sr$ between Equidae and Bovidae enamel is 0.20 ‰. Further research is needed to determine whether the observed isotope differences between Equidae and Bovidae – serving as proxies for hindgut and foregut fermenters, respectively – are primarily driven by diet, digestive physiology, or a combination of both. We note here that the Hippopotamidae and Camelidae are families of polygastric animals with a three-chambered stomach, still their $\delta^{88}Sr$ plots together with the four-chambered stomach ruminants (i.e. Bovidae). In this regard, however, our dataset is insufficient to provide robust constraints on ruminant vs. non-ruminant polygastric animals.

A few non-mutually exclusive interpretative frameworks can be outlined to try to explain the diverse $\delta^{88}Sr$ ratio between monogastric and polygastric herbivores.

1) Rumen absorption: Sr chemical behavior mimics calcium in the body, with site and efficiency of Sr absorption that might differ between species. Ruminants absorb Ca (and Sr) in the small intestine – similarly to monogastric animals – yet some absorption might occur in the rumen (Hyde et al., 2019). These physiological differences could lead to systematic isotope variations between monogastric and polygastric herbivores.
2) Microbial interaction: polygastric animals have complex, multi-chambered stomachs where microbial fermentation tends to precede absorption (Karasov and Douglas, 2013; Membrive, 2016). The microbial populations in polygastrics may influence Sr isotope behavior, potentially through complexation/binding to organic matter, with potential resulting isotope effects on Sr isotopes. Thus, the long food-microbial interaction may enhance selective discrimination against heavier Sr isotopes (^{88}Sr), leading to a lower $^{88}Sr/^{86}Sr$ ratio in polygastric animal tissues.
3) Food retention time: different retention times of food in the different digestive compartments of monogastric vs. polygastric herbivores (Stevens and Hume, 1998) may result in different fractionation pathways. For example, the mean retention time of hay particles for modern horses is ~25 h, while for oxen is ~55 h. Notably, the mean retention time of hay/grain particles for modern pigs is ~48 h, more similar to polygastric oxen than monogastric horses.
4) Incomplete digestion: pH variations and digestion efficiency among monogastric and polygastric herbivores (Dijkstra et al., 2012) may lead to incomplete or differential release of strontium isotopes from plant tissues, potentially resulting in apparent isotope fractionations of animals' tissues. This can also eventually lead to minimally different $^{87}Sr/^{86}Sr$ ratios, if complex plant mixtures are differentially digested/absorbed within the animal digestive system (see Fig. 7).

5. Conclusions

In this study we analyzed fossil dental samples of herbivores (Equidae, Elephantidae, Rhinocerotidae, Suidae, Bovidae, Hippopotamidae and Camelidae) from Tighennif (~1.2–1 Ma, Algeria) with a multi-isotope approach ($\delta^{13}C_{VPDB}$, $\delta^{18}O_{VPDB}$, $\delta^{88}Sr_{NIST987}$ and $^{87}Sr/^{86}Sr$) to investigate the paleoecology of these taxa, with a main focus on $\delta^{88}Sr$ fractionation. C and O indicated an environment composed of a C_3 biomass, with Hippopotamidae standing out as outliers isotopically, possibly due to specific food habits or physiology likely related to their semi-aquatic lifestyle. $^{87}Sr/^{86}Sr$ indicated either limited mobility for the taxa considered or a relatively invariant isotope signature of the local Sr pool, possibly driven by a homogeneous geology. $\delta^{88}Sr$ values of dental enamel specimens are negative, indicative of a likely biogenic signature preserved, while dentine values are shifted of about ~0.23 ‰ toward higher values, possibly indicating diagenetic uptake of Sr. Future comparisons between this isotope ratio and microchemical assessments of tooth preservation (e.g. Gatti et al., 2022; Simpson et al., 2023) could provide valuable insights into the diagenetic processes influencing Sr isotopes.

We observed differences in $\delta^{88}Sr$ enamel values among families, possibly indicating different food end-members with different $\delta^{88}Sr$ ratios. Yet, we propose that at least part of the observed variability is driven by physiological differences among taxa. Specifically, we suggest that monogastric and polygastric herbivores may retain different $\delta^{88}Sr$ ratios due to specific features of their digestive systems and/or their diet.

The $\delta^{88}Sr$ ratio of fossil tooth enamel may serve as a reliable proxy for inferring digestive physiology and dietary differences in extinct and extant terrestrial herbivores, provided the values are of biogenic origin. Its distinctive isotopic signature also offers a valuable tool for identifying diagenetic alterations in bioapatite, as post-depositional processes typically shift $\delta^{88}Sr$ values of terrestrial vertebrate bioapatite toward positive signatures, compared to the typical biogenic negative $\delta^{88}Sr$ values.

CRediT authorship contribution statement

Elena Armaroli: Methodology, Formal analysis, Writing – review &

editing. **Razika Chelli Cheheb:** Resources, Investigation, Writing – review & editing. **Anna Cipriani:** Validation, Supervision, Funding acquisition, Writing – review & editing. **Sara Bernardini:** Methodology, Formal analysis, Writing – review & editing. **Jan van der Made:** Resources, Investigation, Writing – review & editing. **Isabel Cáceres:** Resources, Investigation, Writing – review & editing. **Mohamed Sahnouni:** Supervision, Resources, Project administration, Investigation, Funding acquisition, Conceptualization, Writing – review & editing. **Federico Lugli:** Visualization, Validation, Supervision, Software, Resources, Methodology, Investigation, Funding acquisition, Formal analysis, Data curation, Conceptualization, Writing – original draft.

Declaration of competing interest

The authors declare that they have no known competing financial interests or personal relationships that could have appeared to influence the work reported in this paper.

Acknowledgments

Fieldwork and related research at the site of Tighennif (Algeria) are carried out with a permit attributed to MS by the Algerian Ministry of Culture and Arts, and are funded with grants awarded to MS by Centre National de Recherches Préhistoriques, Anthropologiques et Historiques (CNRPAH) (Algeria), MICIU ([PGC2018-095489-B-I00; PID2022-137070NB-I00] (Spain), The L.S.B. Leakey Foundation (USA), and Fundacion Palarq (Spain). Administrative and logistic support during fieldwork were provided by CNRPAH, the Wilaya of Mascara, the municipality of Tighennif, and the Association of Palikao Man of Tighennif. IC acknowledges the MICINN-PID2021-122355NB-C32, the 2021 SGR 01238 (AGAUR) and the 2023PFR-URV-01238 (URV) projects. Analytical costs were covered by the internal funds of the Metallomics and Geochemistry Research lab (MeGic; https://www.geochem.unimore.it/) of the Department of Chemical and Geological Sciences of UNIMORE. Irene Pennella is thanked for helping during sample preparation for isotope analysis.

Appendix A. Supplementary data

Supplementary data to this article can be found online at https://doi.org/10.1016/j.palaeo.2025.113226.

Data availability

The authors confirm that all data necessary for supporting the scientific findings of this paper have been provided.

References

Andrews, M.G., Jacobson, A.D., Lehn, G.O., Horton, T.W., Craw, D., 2016. Radiogenic and stable Sr isotope ratios ($^{87}Sr/^{86}Sr$, $\delta^{88/86}Sr$) as tracers of riverine cation sources and biogeochemical cycling in the Milford Sound region of Fiordland, New Zealand. Geochim. Cosmochim. Acta 173, 284–303.
Arambourg, C., Hoffstetter, R., 1963. Le gisement de Ternifine: I. Archives de l'Institut de Paléontologie Humaine. Mémoire 32. Paris Inst. Paléontologie Hum.
Argentino, C., Lugli, F., Cipriani, A., Panieri, G., 2021. Testing miniaturized extraction chromatography protocols for combined $^{87}Sr/^{86}Sr$ and $\delta^{88/86}Sr$ analyses of pore water by MC-ICP-MS. Limnol. Oceanogr. Methods 19, 431–440.
Armaroli, E., Lugli, F., Cipriani, A., Tütken, T., 2024. Spatial ecology of moose in Sweden: combined Sr-OC isotope analyses of bone and antler. PLoS One 19, e0300867.
Balout, L., 1955. Préhistoire de l'Afrique du Nord. Paris Arts Métiers Graph.
Balter, V., Simon, L., 2006. Diet and behavior of the Saint-Césaire Neanderthal inferred from biogeochemical data inversion. J. Hum. Evol. 51, 329–338.
Balter, V., Telouk, P., Reynard, B., Braga, J., Thackeray, F., Albarède, F., 2008. Analysis of coupled Sr/ca and $^{87}Sr/^{86}Sr$ variations in enamel using laser-ablation tandem quadrupole-multicollector ICPMS. Geochim. Cosmochim. Acta 72, 3980–3990.
Bekkoussa, B., Meddi, M., Jourde, H., 2008. Forçage climatique et anthropique sur la ressource en eau souterraine d'une région semi-aride: cas de la plaine de Ghriss (Nord-Ouest algérien). Sécheresse 18, 173–184.
Bekkoussa, B., Jourde, H., Batiot-Guilhe, C., Meddi, M., Khaldi, A., Azzaz, H., 2013. Origin of salinity and principal major elements in the Plio-Quaternary aquifer of the Ghriss plain, Northwest Algeria. Hydrol. Sci. Jl 58 (5), 1111–1127.
Bentley, R.A., 2006. Strontium isotopes from the earth to the archaeological skeleton: a review. J. Archaeol. Method Theory 13, 135–187.
Bocherens, H., Koch, P.L., Mariotti, A., Geraads, D., Jaeger, J.-J., 1996. Isotopic biogeochemistry (13 C, 18 O) of mammalian enamel from African Pleistocene hominid sites. Palaios 306–318.
Britton, K., Grimes, V., Dau, J., Richards, M.P., 2009. Reconstructing faunal migrations using intra-tooth sampling and strontium and oxygen isotope analyses: a case study of modern caribou (*Rangifer tarandus granti*). J. Archaeol. Sci. 36, 1163–1172.
Bullen, T., Chadwick, O., 2016. Ca, Sr and Ba stable isotopes reveal the fate of soil nutrients along a tropical climosequence in Hawaii. Chem. Geol. 422, 25–45.
Burton, J.H., Price, D.T., Middleton, W.D., 1999. Correlation of Bone Ba/ca and Sr/ca due to Biological Purification of Calcium. J. Archaeol. Sci. 26, 609–616.
Carscadden, K.A., Emery, N.C., Arnillas, C.A., Cadotte, M.W., Afkhami, M.E., Gravel, D., Livingstone, S.W., Wiens, J.J., 2020. Niche breadth: causes and consequences for ecology, evolution, and conservation. Q. Rev. Biol. 95, 179–214.
Cerling, T.E., Harris, J.M., MacFadden, B.J., Leakey, M.G., Quade, J., Eisenmann, V., Ehleringer, J.R., 1997. Global vegetation change through the Miocene/Pliocene boundary. Nature 389, 153–158.
Cerling, T.E., Harris, J.M., Passey, B.H., 2003. Diets of East African Bovidae based on stable isotope analysis. J. Mammology 84, 456–470.
Cerling, T.E., Harris, J.M., Hart, J.A., Kaleme, P., Klingel, H., Leakey, M.G., Levin, N.E., Lewison, R.L., Passey, B.H., 2008. Stable isotope ecology of the common hippopotamus. J. Zool. 276, 204–212.
Cerling, T.E., Andanje, S.A., Blumenthal, S.A., Brown, F.H., Chritz, K.L., Harris, J.M., Hart, J.A., Kirera, F.M., Kaleme, P., Leakey, L.N., 2015. Dietary changes of large herbivores in the Turkana Basin, Kenya from 4 to 1 Ma. Proc. Natl. Acad. Sci. 112, 11467–11472.
Chelli Cheheb, R., 2018. Les vertébrés fossiles des sites paléolithiques inférieurs: Pirro Nord 13 (Mode I, Italie) et Tighennif (Acheuléen, Algérie). Etude taphonomique et archéozoologique. Università degli Studi di Ferrara.
Clauss, M., Schwarm, A., Ortmann, S., Alber, D., Flach, E.J., Kühne, R., Hummel, J., Streich, W.J., Hofer, H., 2004. Intake, ingesta retention, particle size distribution and digestibility in the hippopotamidae. Comp. Biochem. Physiol. Part A Mol. Integr. Physiol. 139, 449–459.
Copeland, S.R., Cawthra, H.C., Fisher, E.C., Lee-Thorp, J.A., Cowling, R.M., Le Roux, P.J., Hodgkins, J., Marean, C.W., 2016. Strontium isotope investigation of ungulate movement patterns on the Pleistocene Paleo-Agulhas plain of the Greater Cape floristic region, South Africa. Quat. Sci. Rev. 141, 65–84.
D'Angela, D., Longinelli, A., 1990. Oxygen isotopes in living mammal' s bone phosphate: further results. Chem. Geol. 86, 75–82.
Del Valle, H., Rodríguez-Navarro, A.B., Moclán, A., García-Medrano, P., Cáceres, I., 2025. Bone diagenesis and stratigraphic implications from Pleistocene karst systems. Sci. Rep. 15, 5496.
Dijkstra, J., Ellis, J.L., Kebreab, E., Strathe, A.B., López, S., France, J., Bannink, A., 2012. Ruminal pH regulation and nutritional consequences of low pH. Anim. Feed Sci. Technol. 172, 22–33.
Ericson, J., 1985. Strontium isotope characterization in the study of prehistoric human ecology. J. Hum. Evol. 14, 503–514.
Fannin, L.D., Yeakel, J.D., Venkataraman, V.V., Seyoum, C., Geraads, D., Fashing, P.J., Nguyen, N., Fox-Dobbs, K., Dominy, N.J., 2021. Carbon and strontium isotope ratios shed new light on the paleobiology and collapse of Theropithecus, a primate experiment in graminivory. Palaeogeogr. Palaeoclimatol. Palaeoecol. 572, 110393.
Faure, G., Mensing, T.M., 2005. Isotopes: Principles and Applications, 3rd ed. John Wiley & Sons, Hoboken, New Jersey.
France, C.A.M., Thomas, D.B., Doney, C.R., Madden, O., 2014. FT-Raman spectroscopy as a method for screening collagen diagenesis in bone. J. Archaeol. Sci. 42, 346–355.
Gatti, L., Lugli, F., Sciutto, G., Zangheri, M., Prati, S., Mirasoli, M., Silvestrini, S., Benazzi, S., Tütken, T., Douka, K., 2022. Combining elemental and immunochemical analyses to characterize diagenetic alteration patterns in ancient skeletal remains. Sci. Rep. 12, 5112.
Griffith, J.I., James, H.F., Ordoño, J., Fernández-Crespo, T., Gerritzen, C.T., Cheung, C., Spros, R., Claeys, P., Goderis, S., Veselka, B., 2025. Reconstructing prehistoric lifeways using multi-Isotope analyses of human enamel, dentine, and bone from Legaire Sur, Spain. PLoS One 20, e0316387.
Guiserix, D., Albalat, E., Ueckermann, H., Davechand, P., Iaccheri, L.M., Bybee, G., Badenhorst, S., Balter, V., 2022. Simultaneous analysis of stable and radiogenic strontium isotopes in reference materials, plants and modern tooth enamel. Chem. Geol. 606, 121000.
Guiserix, D., Dodat, P.-J., Jaouen, K., Albalat, E., Cardoso, J.M., Maureille, B., Balter, V., 2024. Stable isotope composition and concentration systematics of ca and trace elements (Zn, Sr) in single aliquots of fossil bone and enamel. Geochim. Cosmochim. Acta 367, 123–132.
Hajj, F., Poszwa, A., Bouchez, J., Guérold, F., 2017. Radiogenic and "stable" strontium isotopes in provenance studies: a review and first results on archaeological wood from shipwrecks. J. Archaeol. Sci. 86, 24–49.
Hartmann, J., Moosdorf, N., 2012. The new global lithological map database GLiM: a representation of rock properties at the Earth surface. Geochem. Geophys. Geosyst. 13, Q12004.
Heuser, A., Tütken, T., Gussone, N., Galer, S.J.G., 2011. Calcium isotopes in fossil bones and teeth — Diagenetic versus biogenic origin. Geochim. Cosmochim. Acta 75, 3419–3433.

Hyde, M.L., Wilkens, M.R., Fraser, D.R., 2019. In vivo measurement of strontium absorption from the rumen of dairy cows as an index of calcium absorption capacity. J. Dairy Sci. 102, 5699–5705.
Karasov, W.H., Douglas, A.E., 2013. Comparative digestive physiology. Compr. Physiol. 3, 741–783.
Knudson, K.J., Williams, H.M., Buikstra, J.E., Tomczak, P.D., Gordon, G.W., Anbar, A.D., 2010. Introducing $\delta^{88/86}$Sr analysis in archaeology: a demonstration of the utility of strontium isotope fractionation in paleodietary studies. J. Archaeol. Sci. 37, 2352–2364.
Koutamanis, D., McCurry, M., Tacail, T., Dosseto, A., 2023. Reconstructing Pleistocene Australian herbivore megafauna diet using calcium and strontium isotopes. R. Soc. Open Sci. 10, 230991.
Kowalik, N., Anczkiewicz, R., Müller, W., Spötl, C., Bondioli, L., Nava, A., Wojtal, P., Wilczyński, J., Koziarska, M., Matyszczak, M., 2023. Revealing seasonal woolly mammoth migration with spatially-resolved trace element, Sr and O isotopic records of molar enamel. Quat. Sci. Rev. 306, 108036.
Kubat, J., Nava, A., Bondioli, L., Dean, M.C., Zanolli, C., Bourgon, N., Bacon, A.-M., Demeter, F., Peripoli, B., Albert, R., 2023. Dietary strategies of Pleistocene Pongo sp. and Homo erectus on Java (Indonesia). Nat. Ecol. Evol. 7, 279–289.
Levin, N.E., Cerling, T.E., Passey, B.H., Harris, J.M., Ehleringer, J.R., 2006. A stable isotope aridity index for terrestrial environments. Proc. Natl. Acad. Sci. 103, 11201–11205.
Lewis, J., Pike, A.W.G., Coath, C.D., Evershed, R.P., 2017. Strontium concentration, radiogenic (^{87}S/^{86}Sr) and stable (δ^{88}Sr) strontium isotope systematics in a controlled feeding study. STAR Sci. Technol. Archaeol. Res. 3, 53–65.
Lugli, F., Cipriani, A., Peretto, C., Mazzucchelli, M., Brunelli, D., 2017. In situ high spatial resolution ^{87}Sr/^{86}Sr ratio determination of two Middle Pleistocene (c.a. 580 ka) *Stephanorhinus hundsheimensis* teeth by LA–MC–ICP–MS. Int. J. Mass Spectrom. 412, 38–48.
Lugli, F., Sciutto, G., Oliveri, P., Malegori, C., Prati, S., Gatti, L., Silvestrini, S., Romandini, M., Catelli, E., Casale, M., Talamo, S., Iacumin, P., Benazzi, S., Mazzeo, R., 2021. Near-infrared hyperspectral imaging (NIR-HSI) and normalized difference image (NDI) data processing: an advanced method to map collagen in archaeological bones. Talanta 226, 122126.
Luz, B., Kolodny, Y., Horowitz, M., 1984. Fractionation of oxygen isotopes between mammalian bone-phosphate and environmental drinking water. Geochim. Cosmochim. Acta 48, 1689–1693.
Martin, J.E., Tacail, T., Cerling, T.E., Balter, V., 2018. Calcium isotopes in enamel of modern and Plio-Pleistocene East African mammals. Earth Planet. Sci. Lett. 503, 227–235.
McArthur, J.M., Howarth, R.J., Bailey, T.R., 2001. Strontium isotope stratigraphy: LOWESS version 3: best fit to the marine Sr-isotope curve for 0–509 Ma and accompanying look-up table for deriving numerical age. J. Geol. 109, 155–170.
Membrive, C.M.B., 2016. Anatomy and physiology of the Rumen. In: Rumenology. Springer Nature, pp. 1–38.
Michailow, M.M., Lugli, F., Cipriani, A., Della Giustina, F., Ferretti, A., Malferrari, D., Fowler, D., Fowler, E.F., Weber, M., Tütken, T., 2025. Combined Ca, Sr isotope and trace element analyses of late cretaceous dinosaur teeth: assessing diet versus diagenesis. Geochim. Cosmochim. Acta. https://doi.org/10.1016/j.gca.2025.05.006.
Müller, W., Lugli, F., McCormack, J., Evans, D., Anczkiewicz, R., Bondioli, L., Nava, A., 2024. Human life histories. In: Treatise on Geochemistry, Third edition. Elsevier, pp. 281–328.
Niehaus, A.J., Mora, D.P., 2022. Digestive system and abdomen. In: Medicine and Surgery of Camelids. Wiley, pp. 336–390.
Nielsen, S.P., 2004. The biological role of strontium. Bone 35, 583–588.
Nitzsche, K.N., Wakaki, S., Yamashita, K., Shin, K., Kato, Y., Kamauchi, H., Tayasu, I., 2022. Calcium and strontium stable isotopes reveal similar behaviors of essential ca and nonessential Sr in stream food webs. Ecosphere 13, e3921.
Oeser, R.A., von Blanckenburg, F., 2020. Strontium isotopes trace biological activity in the critical Zone along a climate and vegetation gradient. Chem. Geol. 558, 119861.
O'Leary, M.H., 1981. Carbon isotope fractionation in plants. Phytochemistry 20, 553–567.
Pederzani, S., Britton, K., 2019. Oxygen isotopes in bioarchaeology: principles and applications, challenges and opportunities. Earth-Sci. Rev. 188, 77–107.
Pellegrini, M., Donahue, R.E., Chenery, C., Evans, J., Lee-Thorp, J., Montgomery, J., Mussi, M., 2008. Faunal migration in late-glacial Central Italy: implications for human resource exploitation. Rapid Commun. Mass Spectrom. 22, 1714–1726.
Radloff, F.G.T., Mucina, L., Bond, W.J., Le Roux, P.J., 2010. Strontium isotope analyses of large herbivore habitat use in the Cape Fynbos region of South Africa. Oecologia 164, 567–578.
Reynard, L.M., Henderson, G.M., Hedges, R.E.M., 2010. Calcium isotope ratios in animal and human bone. Geochim. Cosmochim. Acta 74, 3735–3750.
Romaniello, S.J., Field, M.P., Smith, H.B., Gordon, G.W., Kim, M.H., Anbar, A.D., 2015. Fully automated chromatographic purification of Sr and ca for isotopic analysis. J. Anal. At. Spectrom. 30, 1906–1912.
Sahnouni, M., van der Made, J., 2009. The Oldowan in North Africa within a biochronological framework. In: Schick, K., Toth, N. (Eds.), The Cutting Edge: New Approaches to the Archaeology of Human Origins. Stone Age Institute Press, Bloomington, pp. 179–210.
Saidani, N., 2023. Les microvertébrés du site à hominidés de Tighennif (Ex, Ternifine, Algérie) Taxonomie, taphonomie et paléoécologie. Universitat Rovira i Virgili, Tarragona.
Shrader, A.M., Owen-Smith, N., Ogutu, J.O., 2006. How a mega-grazer copes with the dry season: food and nutrient intake rates by white rhinoceros in the wild. Funct. Ecol. 376–384.
Simpson, E.M.B., Crowley, B.E., Sturmer, D.M., 2023. Is the damage worth it? Testing handheld XRF as a non-destructive analytical tool for determining biogenic bone and tooth chemistry prior to destructive analyses. Front. Environ. Archaeol. 1, 1098403.
Skulan, J., DePaolo, D.J., 1999. Calcium isotope fractionation between soft and mineralized tissues as a monitor of calcium use in vertebrates. Proc. Natl. Acad. Sci. USA 96, 13709–13713.
Stevens, C.E., Hume, I.D., 1998. Contributions of microbes in vertebrate gastrointestinal tract to production and conservation of nutrients. Physiol. Rev. 78, 393–427.
Thomas, D.B., McGoverin, C.M., Fordyce, R.E., Frew, R.D., Gordon, K.C., 2011. Raman spectroscopy of fossil bioapatite—a proxy for diagenetic alteration of the oxygen isotope composition. Palaeogeogr. Palaeoclimatol. Palaeoecol. 310, 62–70.
Tütken, T., Held, P., Herrmann, S., Galer, S., 2015. Combined $\delta^{88/86}$Sr and ^{87}Sr/^{86}Sr in bones and teeth: A toolbox for diet and habitat reconstruction. In: In: 25th Anniversary of the Goldschmidt Conference, Prague, 16th-21st August. Abstract.
Wall, W.P., 1983. The correlation between high limb-bone density and aquatic habits in recent mammals. J. Paleontol. 57, 197–207.
Weber, M., Lugli, F., Jochum, K.P., Cipriani, A., Scholz, D., 2018. Calcium carbonate and phosphate reference materials for monitoring bulk and microanalytical determination of Sr isotopes. Geostand. Geoanal. Res. 42, 77–89.
Weber, M., Weber, K., Winkler, D.E., Tütken, T., 2025. Calcium and strontium isotopes in extant diapsid reptiles reflect dietary tendencies—a reference frame for diet reconstructions in the fossil record. Proc. B 292, 20242002.
Wooller, M.J., Bataille, C., Druckenmiller, P., Erickson, G.M., Groves, P., Haubenstock, N., Howe, T., Irrgeher, J., Mann, D., Moon, K., 2021. Lifetime mobility of an Arctic woolly mammoth. Science 373, 806–808.
Wu, N., Zhang, J., Mao, H., Zhang, G., Zhao, Z., 2024. Geochemical behavior of stable strontium isotopes during continental weathering process: a review. Geosyst. Geoenviron. 3, 100144.